applied sciences

MDPI

Article

Design and Implementation of a Tether-Powered Hexacopter for Long Endurance Missions

Kai-Hung Chang and Shao-Kang Hung *

Department of Mechanical Engineering, National Yang Ming Chiao Tung University, No. 1001, University Road, Hsinchu 30010, Taiwan; mxc0451002.me04g@nctu.edu.tw

* Correspondence: skhung@nctu.edu.tw; Tel.: +886-3571-2121 (ext. 55115)

Abstract: A tether-powered unmanned aerial vehicle is presented in this article to demonstrate the highest altitude and the longest flight time among surveyed literature. The grid-powered ground station transmits high voltage electrical energy through a well-managed conductive tether to a 2-kg hexacopter hovering in the air. Designs, implementations, and theoretical models are discussed in this research work. Experimental results show that the proposed system can operate over 50 m for 4 h continuously. Compared with battery-powered multicopters, tether-powered ones have great advantages on specific-area long-endurance applications, such as precision agriculture, intelligent surveillance, and vehicle-deployed cellular sites.

Keywords: unmanned aerial vehicle; power transmission; optimal design

Citation: Chang, K.-H.; Hung, S.-K. Design and Implementation of a Tether-Powered Hexacopter for Long Endurance Missions. *Appl. Sci.* **2021**, *11*, 11887. https://doi.org/10.3390/app112411887

Academic Editors: Martin Saska, Giancarmine Fasano and Wojciech Giernacki

Received: 1 November 2021
Accepted: 7 December 2021
Published: 14 December 2021

1. Introduction

Endurance is a crucial performance index of electrical rotary-wing unmanned aerial vehicles (UAV). Intuitively, bigger batteries lead to longer flight time; however, lifting heavy batteries requires more electricity and thus decreases the endurance. Therefore, an optimal battery capacity exists to achieve the maximum endurance. The endurance of battery-powered UAVs has been investigated thoroughly [1–6]. Methods of increasing maximum endurance can also be found in [7–15]. Methods of increasing maximum endurance include optimizing the design of UAVs according to their applications [8–11], deposition of empty batteries [6,7], reducing energy loss and cost during operation [12,13], and combining with other energy sources [14,15]. The performance of typical battery-powered UAVs is summarized in Table 1.

For several applications, such as precision smart agriculture, intelligent surveillance, and temporary telecom hotspots, for emergencies which require UAV working within a specific area for a long time, tether-powered UAVs have a great potential to demonstrate much longer endurance than battery-powered UAVs.

A tether-powered UAV usually contains a multicopter in the air and a ground station, with a conductive tether connecting both of them [16,17]. The electrical power is transmitted form the ground station to the multicopter. Tether-powered multicopters are able to extend their endurance to "near infinite" since the ground station is powered by the grid, a fuel generator, or a huge battery that contains much more energy than can be lifted in the air. In previous researches, a tether-powered multicopter can either be directly powered by a tether [16,18,19] or through an additional electricity converter installed onboard [17,20,21]. Usually, one with an electrical converter is able to achieve longer tether length than those being directly powered by a tether. Tether-powered multicopters can operate with only small batteries onboard or no battery at all. Onboard batteries only serve as a backup power to prevent a possible multicopter crash in case of power failure [22,23]. Several researches on the power tether can be found in [18,19,21,24]. Our previous work provides a math model to optimize tether parameters for different missions [18]. A power-over-tether system is presented to control the tether tension automatically [19]. A tether structure that

can transmit both power and data is invented in [21]. An optimum design of multi-core tether to transmit AC power while considering the skin effect is introduced in [24], but skin effect is not an issue for our DC-powered UAV.

Table 1. Performance of typical battery-powered UAVs.

Reference	Rotors	Power Source	Battery Capacity (mAh)	Weight w/o Battery (g)	Altitude (m)	Max Endurance (Min)	Remark
[2] Wanze	4	7.4 V Battery	8000	119	NA	34	
[2] Ninja	4	11.1 V Battery	2000	352	NA	15	
[3]	4	11.1 V Battery	2200	~359	1.5–2.5	17.8	
[4]	6	14.8 V Battery	40,000	2000	NA	29.24	
[6]	4	11.1 V Battery	2300	~360	NA	19	Releasing empty battery
[8]	4	Battery (voltage NA)	2100	416	1–2.5	Battery only: 14 Battery + magnet: 102	Using magnets to attach to the ceiling
[9]	6	11.1 V Battery	3471	3294	NA	36	
[11]	4	3.7 V Battery	650	32	NA	31	
[14]	8	22.2 V Battery + Fuel	5200	19,600	NA	60	

This research work focuses on the system design, tether selection, and outdoor implementation. A 4-h mission with the operation altitude up to 50 m will be executed to demonstrate the longest endurance and the highest altitude among surveyed experiments about tether-powered UAVs. The structure of this paper is organized as follows. Section 2 introduces the composition of our tether-powered hexacopter, detailed design parameters, power consumption model, tether selection, and design considerations. Section 3 describes experimental results. Section 4 describes the analysis of test results. Section 5 presents the conclusion of this article and improvements that can be done in the future.

2. Design and Analysis

The system diagram and photos of the proposed tether-powered hexacopter are shown in Figure 1. This system can be divided into two subsystems, the ground station and the aerial vehicle with a mission payload. Both subsystems are connected physically by a tether which transmits electrical power form the ground station to the hexacopter. Navigation signals and telemetry data are transmitted wirelessly through the off-the-shelf radio modules. Flight data are recorded in the flight controller and will be read out and analyzed after every experiment.

2.1. Ground Station

The ground station contains three DC power supplies connected in series, a slip ring, a winch, a tether guider, wireless communicators, and a laptop computer which serves as a mission planner. This ground station can be powered by 220 Vac from the grid or a diesel generator.

Two 750 W/48 V DC power supplies (RSP-750-48, Mean Well, Taiwan) and a 1500 W voltage adjustable DC power supply (KXN-3050D, Zhaoxin, China) are capable of providing maximum 15.7 A current and maximum 120 V DC voltage to the slip ring (M022A-06, Senring, China), which conducts electricity to the tether when the winch is rotating. The winch is controlled by a 100 W industrial AC servo motor (FRMS1020604D, Hiwin, Taiwan) under a constant torque mode to maintain a suitable tension of the tether. The torque reference is set according to the status of flight. The angular speed of the winch is limited under 200 rpm to protect the slip ring. A tether guider is installed in front of the winch to help tether accumulate uniformly on the spool. The winch controls are detailed in

Appendix A. Telemetry data is received by a laptop and decoded by software "Mission Planner". The hexacopter is navigated manually through a radio transmitter.

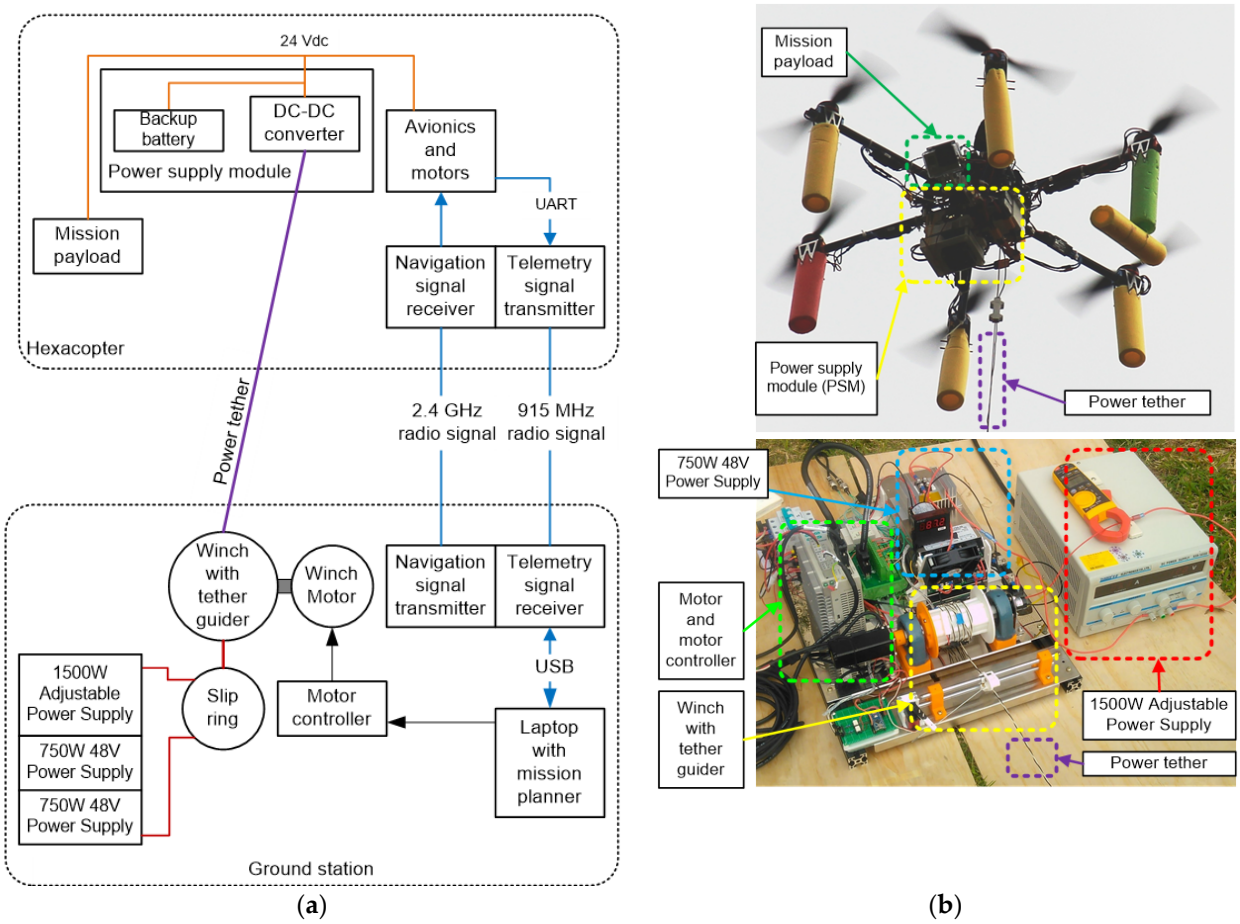

Figure 1. (**a**) System diagram of Tether-powered hexacopter; (**b**) Photos of hexacopter and ground station.

2.2. Hexacopter

The hexacopter subsystem is built with off-the-shelf components listed in Table 2. Its airframe has 2000 g weight and it has the ability to carry a 1500 g payload because the heavy battery is omitted. The payload of the following experiments is an action camera (Hero3+, GoPro) with 170 g weight. Its mission is to periodically take videos/photos of the target site which will later be turned into a time-lapse video. The payload module can be changed to others according to mission needs.

Instead of being powered by a large battery, the hexacopter is powered by a 600 W custom-built DC-DC converter (based on LTC3871, Analog Devices) which receives high voltage from the tether and delivers a controlled constant 24 V to every component on the hexacopter. The details of the DC-DC converter, including its topology, efficiency, and the feedback control circuit are supplemented in Appendix B.

As shown in Figure 2a, an aluminum heatsink and two fans dissipate the heat generated by the DC-DC converter. Figure 2b is the thermal image of the DC-DC convertor providing 30 A at 24 V. The hottest region occurs at the location of high side MOSFETs at 86.8 °C, which is within their safe range.

Table 2. Specifications of the proposed hexacopter subsystem.

Specifications	Description
Weight of airframe	2000 g
Hub-to-hub (diagonal) dimension	680 mm
Flight controller (avionics)	3DR Pixhawk with ArduPilot
Electrical speed controller (ESC)	Hobbywing Platinum 30A Pro 2-6S ESC
Brushless DC Motor	SunnySky V3508-29 KV380
Propeller	1255 carbon fiber propeller
Telemetry	915 MHz transmitter
Power consumption by Avionics	10 W approximately
Weight of power supply module (PSM)	696 g
Nominal output voltage of PSM	24 V
Nominal output power of PSM	600 W
Energy capacity of backup battery	36 Wh
Payload capacity	1500 g
Weight of mission payload	170 g
Power consumption by mission payload	Less than 5 W

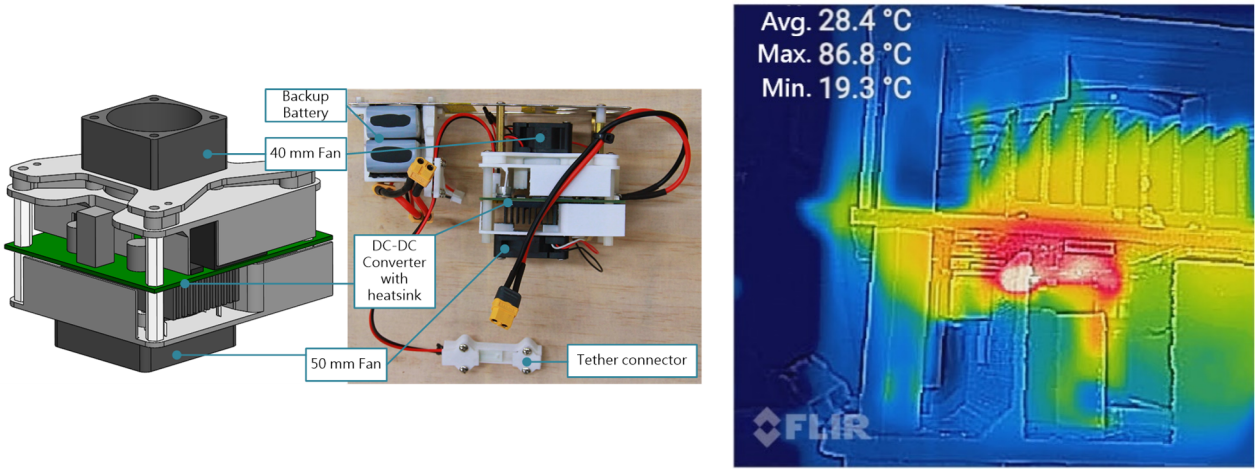

(**a**) (**b**)

Figure 2. (**a**) The power supply module (PSM) consists of a DC-DC convertor, a heat sink, cooling fans, and a backup battery for emergency landing; (**b**) The thermal image of the DC-DC convertor providing 30 A at 24 V.

A 36 Wh battery serves as a backup power which provides around 4 min of flight-time to land the hexacopter safely in case of emergency due the malfunction of the power supply chain. This backup battery is pre-charged to 24.1 V and then directly parallel-connected to the DC bus, which is internally controlled at 24 V. After turning on the system, the backup battery gradually discharges to 24 V and then always stays with the DC bus in the following. The experimental data show that the DC bus voltage runs between 23 to 24 V, which will not damage the battery.

2.3. Tether Optimization

The maximum range or altitude of a tether-powered multicopter is limited by the tether length and the power that can be used. Considering the condition where the hexacopter hovers right above the ground station, the length of tether is equal to the altitude. The power needed by the hexacopter, P_n, for hovering in the air can be expressed as Equation (1).

$$P_n = \frac{1}{\eta}\left[n\left[f\left(\frac{W_{IA}}{n}\right)\right] + P_{AV} + P_{PL}\right] \quad (1)$$

where η represents the efficiency of the DC-DC convertor of PSM and is fixed to 0.9307 as the worst case. The symbol n, which is 6 for a hexacopter, represents the quantity of rotors. The function $f(\ )$ represents the thrust-to-power function of a single rotor where the input unit is gram-force and the output unit is Watt. W_{IA} represents the weight in the air. P_{AV} and P_{PL} represent the power consumed by avionics and the payload, respectively. The thrust-to-power function used in this research work is acquired from our test bed described in [18]. The curve fitting with the momentum theory [25] can be described by Equation (2).

$$P_n = \frac{F_r^{\frac{3}{2}}}{\eta_r \sqrt{2\rho_a A_r}} \tag{2}$$

where F_r is the thrust force produced by the rotor, η_r is a figure of merit of the rotor, ρ_a is the density of air, and A_r is the swept area of the propeller. The test data are shown in Figure 3, and the 3/2 order fitted regression becomes Equation (3).

$$f(F_r) = 0.0039 F_r^{\frac{3}{2}} + 1.95 \tag{3}$$

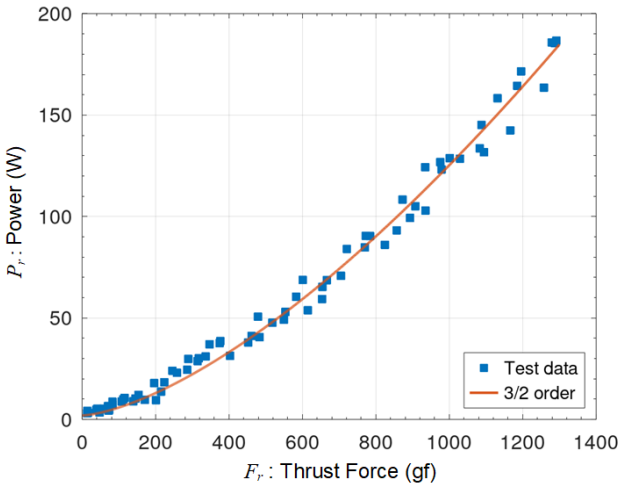

Figure 3. The thrust-to-power function of a single rotor.

A none zero constant 1.95 in Equation (3) implies the static power loss of ESC when the rotor is not rotating.W_{IA} can be represented as

$$W_{IA} = W_{TO} + dH \tag{4}$$

where W_{TO} is the takeoff weight of the hexacopter, d is the tether's weight of per unit length, H is the length of the tether, and dH is the weight of tether in the air. The power submitted by the ground station, P_G, can be expressed as

$$P_G = V_G I_G = {I_G}^2 \rho H + P_r \tag{5}$$

where V_G and I_G represent voltage and current submitted by the ground station respectively. The symbol ρ is the tether's resistivity per unit length thus the power consumed by the tether can be represented as ${I_G}^2 \rho H$. P_r is the residual power that the hexacopter can receive. The maximum power that can be transferred from the ground station to the hexacopter is limited by the minimum allowable input voltage of the DC-DC converter $(V_{DCH,MIN})$. For most DC-DC converters, an under voltage trip is likely to occur if input voltage (V_{DCH}) drops below $V_{DCH,MIN}$. This limitation can be expressed as

$$V_G - I_H \rho H \geq V_{DCH,MIN} \tag{6}$$

With adequate rearrangements, Equations (5) and (6) can be derived as Equation (7), which expresses the power that can be received by the hexacopter, P_r.

$$P_r = \frac{V_{DCH,MIN}(V_G - V_{DCH,MIN})}{\rho H} \tag{7}$$

A long tether containing copper filaments has a significant weight. The lightest option in the market is the 44A012X series (TE connectivity, USA) unshielded, unjacketed, general purpose, 600 V, two conductor 1-pair twisted cable. The weight and resistivity per unit length are listed in Table 3. Substituting these parameters into the above mathematical model, we have Figure 4 showing the overall performance of different tether size in American Wire Gage (AWG). The solid lines, derived by Equation (1), indicate the needed power versus the tether's length. Their slope is positive because more power is needed for hanging a heavier tether in the air. On the other hand, the dash lines, derived by Equation (7), indicate the received power versus the tether's length. Their slope is negative because more voltage is dropped due to the higher resistance. For a certain tether size, the junction of the solid line and the dash line indicates the maximum altitude and its corresponding power, which are summarized in Figure 5.

Table 3. Parameters of the 44A012X series power tether.

Tether Size	Weight per Unit Length (d)	Resistivity per Unit Length (ρ)
10 AWG	103.3 g/m	0.00088 Ω/m
12 AWG	65.9 g/m	0.00568 Ω/m
14 AWG	42.3 g/m	0.00904 Ω/m
16 AWG	26.9 g/m	0.01435 Ω/m
18 AWG	19.8 g/m	0.02095 Ω/m
20 AWG	13.0 g/m	0.03310 Ω/m
22 AWG	8.8 g/m	0.05296 Ω/m
24 AWG	5.9 g/m	0.08422 Ω/m
26 AWG	4.3 g/m	0.15484 Ω/m

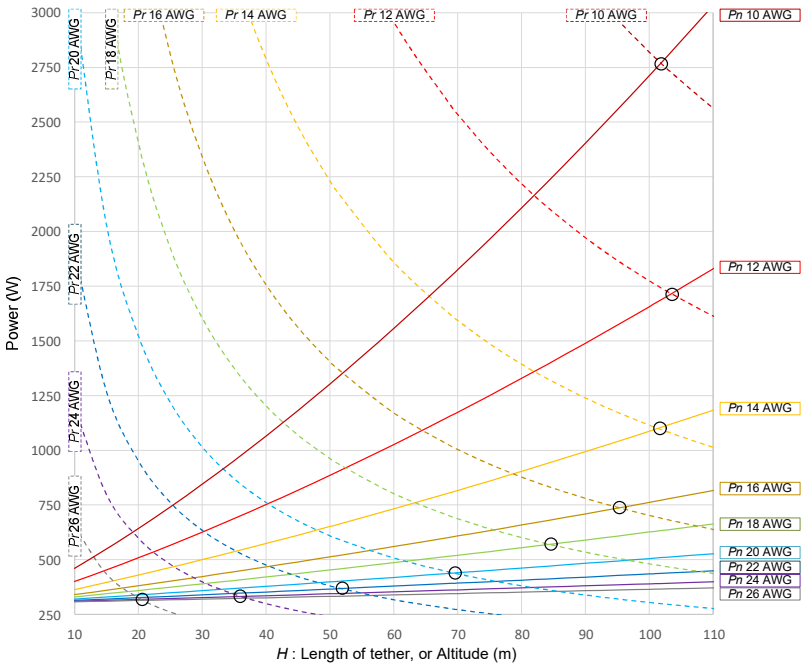

Figure 4. The solid lines indicate the needed power, P_n, versus the tether's length. The dash lines indicate the received power, P_r, versus the tether's length. For a certain tether size, the junction of the solid line and the dash line indicates the maximum altitude and its corresponding power.

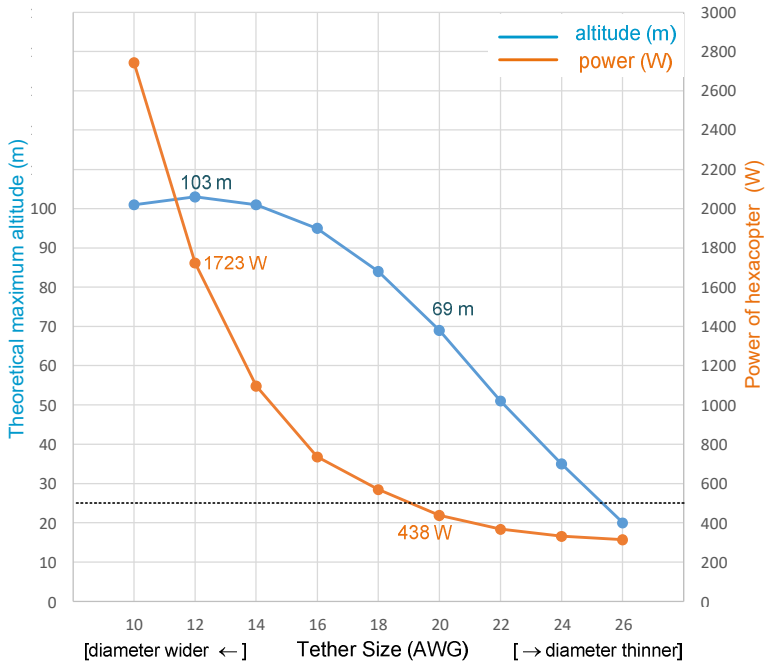

Figure 5. Theoretical maximum altitude and the corresponding power needed and received by the hexacopter for different tether sizes. With the 1723 W power supply, selecting 12 AWG achieves 103 m altitude; with the 438 W power supply, selecting 20 AWG achieves 69 m altitude.

2.4. Margins for Safety

For the proposed system, Figure 5 shows that the optimum tether size is 12 AWG which achieves 103 m theoretical maximum altitude with 1723 W power requirement; however, such a PSM is too heavy to be lifted by the hexacopter. The nominal power output of our PSM is 600 W. Considering an unideal condition with gusts, sidewind, and thermal drift of the mathematical model, we set the power limit at 500 W, the dotted line in Figure 5. Under the safety margin, 20 AWG tether is chosen and equipped for the following experiments. The tether's length should not exceed 69 m, the theoretically achievable boundary.

3. Experimental Results

Two types of tests, namely a functional test and an endurance test, have been executed. Parameters of each test are listed in Table 4. In the functional test, the hexacopter will reach the altitude of 15 m and fly for 30 min. The objective of the functional test is to confirm the whole functionality of the system, rationale of test procedures and gather flight data to verified design parameters. The goal of the endurance test is to prove that the system is capable of "near infinite" air time. The hexacopter will reach the altitude of 50 m and fly for 240 min (4 h) or more to prove such a feature. All experiments were performed outdoors on the campus lawn.

Table 4. Test parameters.

Test Parameter	Functional Test	Endurance Test
Target endurance	30 min	240 min
Target altitude	15 m	50 m
Tether length	26 m	61 m
Ground supply voltage	fixed 90 V	90 V or higher

3.1. Functional Test

Log of functional test is shown in Figure 6. The hexacopter has reached average altitude of 17 m and maximum altitude of 21 m. The PSM provides average 12 A current, 23.5 V voltage, and equivalent to 282 W power consumption. The mission of 50 min has been completed successfully and the functionality of the whole system can be confirmed.

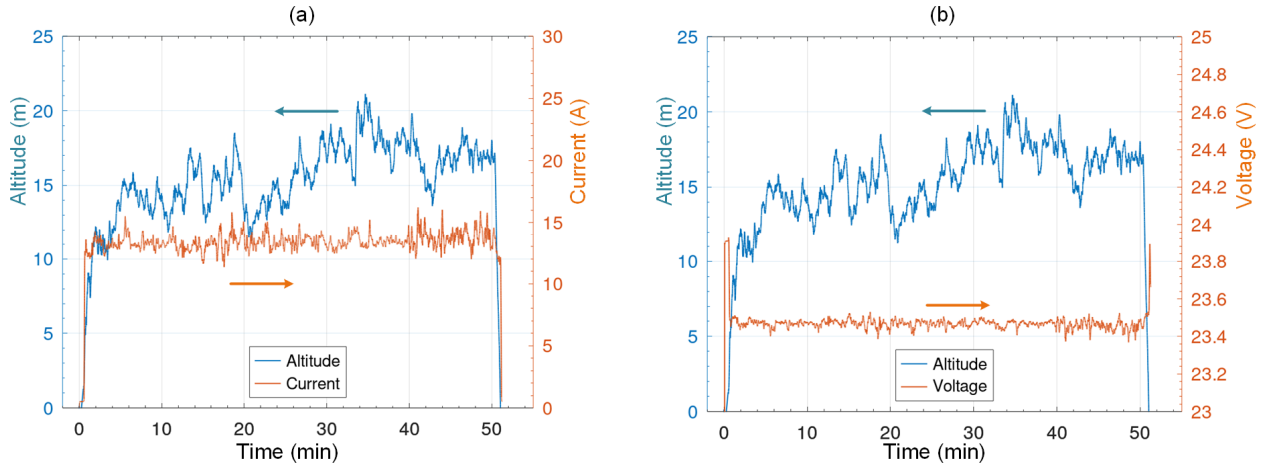

Figure 6. Functional test: (**a**) altitude/current and (**b**) altitude/voltage during 50-min flight.

3.2. Endurance Test

Log of Endurance test is shown in Figure 7. The hexacopter reached average altitude of 48 m and maximum altitude of 59 m. The PSM provides average 17.9 A current, 23.5 V voltage, and is equivalent to 421 W power. The power requirement in the endurance test is more than in the functionality test because the length is much longer. The tether generates significant heat while conducting power from the ground station to the hexacopter. The side wind is also stronger at higher altitudes; therefore, the hexacopter needs more power to stabilize itself. The mission of 240 min has been completed successfully and thus the "near infinite" flight time can be demonstrated with a time-lapse video [26]. Among our surveyed research works so far, no battery powered UAV can fly for longer than 4 h.

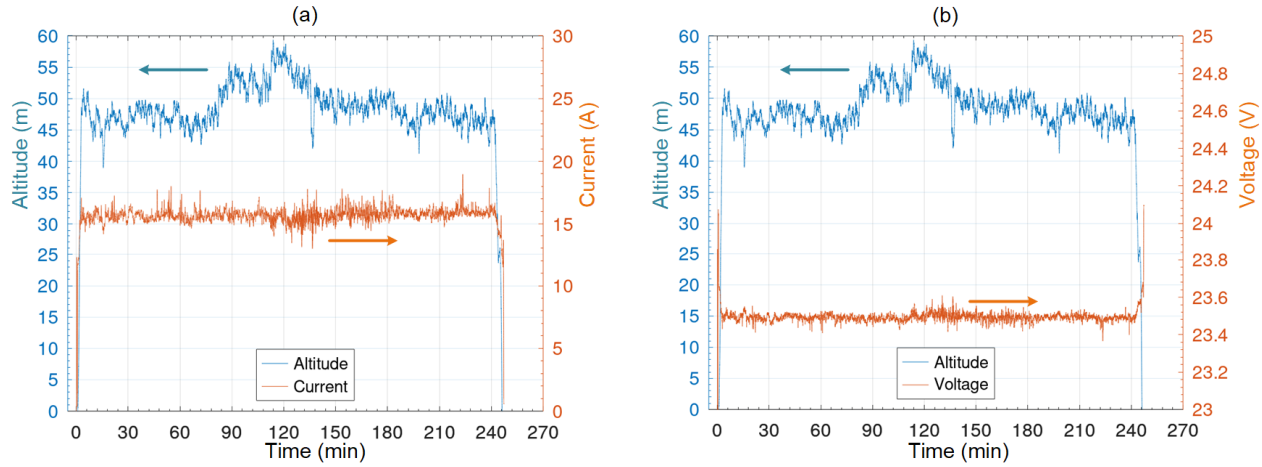

Figure 7. Endurance test: (**a**) altitude/current and (**b**) altitude/voltage during 240-min flight.

Averaged measurement data during the endurance test are listed in Table 5 along with those derived from the model in the previous section. In the endurance test, total tether length in air is 60 m and data are derived based on this length.

Table 5. Endurance test data and data from model.

Item	Value
Measured ground supply voltage	98.1 V
Measured ground supply current	6.6 A
Calculated ground supply power	648 W
Measured tether resistance	4.02 Ω
Calculated power consumption by tether	175 W
Measured power consumption of hexacopter	421 W
Theoretical power consumption of hexacopter	438 W
Theoretical power consumption model inaccuracy	3.88%

4. Discussions

The 421 W power consumption was measured in an outdoor environment with moderate wind, evidenced by our time-lapse experiment video [26]. According to the historical weather records [27], the averaged wind speed was 2.75 m/s at 10 m height over the ground level. Therefore, the 50 m altitude wind speed was estimated at 5 m/s according to the boundary layer theory. Our system was tested at 8 m/s wind speed, and it worked normally. In the future, we will try to equip an anemometer with the UAV to measure the in-situ wind speed. The DC-DC convertor provides 600 W, which implies a 179 W (29.8%) spare. Furthermore, a 36 Wh battery serves as a backup power which provides 4 min of flight-time to land the hexacopter safely in case of an emergency due to the malfunction of the power supply chain. That implies the parallel-connected backup battery can provide extra 540 W power (totally 1140 W), which can satisfy the power requirement due to the strong wind shear and the movement required by the mission. A 3.88% power consumption difference between the theoretical model and measurements is observed. The model inaccuracy could be caused by reasons listed below:

1. The extra forces caused by tether: The force caused by wind and tension on the tether may cause the hexacopter to produce extra thrust in order to balance itself;
2. Imbalance of the hexacopter: Power supply and mission payload may cause an imbalance, thus requiring extra thrust for the hexacopter to maintain its altitude;
3. Side wind: Since the hexacopter is set to hover at a fixed position throughout the test, side wind may cause it to produce more thrust than estimated in order to maintain its position.

5. Conclusions

The proposed tether-powered hexacopter demonstrates successful outdoor operation with an endurance of 4 h at a height of 50 m. This system achieves the longest flight time and the highest altitude among surveyed experiments. A mathematical model is also proposed to estimate the optimal tether's size and its theoretical length limit. The model error is 3.88% compared with the measured data. The reasons may be the extra force exerted by the tether, imbalance of the hexacopter, and the sidewind. The influences of above reasons can be considered in future works to increase model accuracy.

Author Contributions: Conceptualization, S.-K.H.; methodology, S.-K.H. and K.-H.C.; software, K.-H.C.; validation, S.-K.H. and K.-H.C.; formal analysis, K.-H.C.; investigation, S.-K.H. and K.-H.C.; resources, S.-K.H.; data curation, K.-H.C.; writing—original draft preparation, S.-K.H. and K.-H.C.; writing—review and editing, S.-K.H.; visualization, K.-H.C.; supervision, S.-K.H.; project administration, S.-K.H. funding acquisition, S.-K.H. All authors have read and agreed to the published version of the manuscript.

Funding: This research was partially funded by Ministry of Science and Technology, Taiwan, grant number 108-2221-E-009-084-MY2.

Institutional Review Board Statement: Not applicable.

Informed Consent Statement: Not applicable.

Acknowledgments: The authors would like to thank Force Precision Instrument Co. Ltd., Taiwan for technical support.

Conflicts of Interest: The authors declare no conflict of interest.

Appendix A. Details of Winch Control

To prevent tether from dangling and to realize "auto-rewind", the winch motor controller/driver (D2T0423-S, Hiwin, Taiwan) works on constant torque mode. Three flight scenarios namely "Ascend", "Hover and slowly descend" and "Fast descend" are arranged and different torque references are set accordingly. In "Ascend" scenario, the torque value is set to slightly negative so that the hexacopter can pull out tether effortless. In "Hover and low descend" scenario, a positive torque reference is set in order to prevent tether from dangling. In "Fast descend", a relatively greater torque is set so that the rewind speed can catch up hexacopter's descending rate. Torque values are preset into motor controller according to each scenario. The scenario is switched by the operator manually during flight.

Table A1. Details of winch operation.

Flight Scenarios	Ascend	Hover & Slowly Descend	Fast Descend
Reference winch torque * (mNm)	−16	64	160
Maximum winch speed (rpm)	200	200	200
Maximum tether tension * (gf)	−50	201	502
Minimum tether tension * (gf)	−30	118	297

* Positive values mean the winch rewinds the tether backward; negative values mean the winch releases the tether outward.

Appendix B. Details of DC-DC Convertor

The DC-DC convertor equipped on UAVs should be with light weight and high efficiency. We tried to find off-the-shelf ones, but their specifications couldn't satisfy our demand. Therefore, we built our own DC-DC convertor to step-down the high-side tether voltage (~100 V) to a constant low-side voltage 24 V. The most challenging point is that the high-side voltage is time-varying because of the long tether with significant resistance. A bidirectional synchronous buck or boost controller LTC3871 (Analog Devices, USA) is selected because of its high efficiency and unique architecture allows dynamic regulation of input voltage.

The schematic drawing and the photograph of the DC-DC converter's printed circuit board are shown in Figures A1 and A2. The low-side output voltage (LV) is programmed at 24 V by two external feedback resistive dividers, R15 and R16. The divided voltage is fed back via the pin #2 (VFBLow) into the internal control loop, which keep the output voltage at constant 24 V. The switching frequency, maximum input voltage, minimum input voltage, nominal output voltage, nominal output current, and maximum output current are 200 kHz, 96 Vdc, 48 Vdc, 24 Vdc, 25 A, and 30 A, respectively.

Several surface mount MOSFETs are selected because of their small footprint and light weight. They are placed enough separately to avoid heat concentration. Their heat can be conducted to the backside of PCB with vias and dissipates to the air through the thermal conductive pad and the aluminum fin. Two fans are installed on both sides of PCB in order to improve the convection.

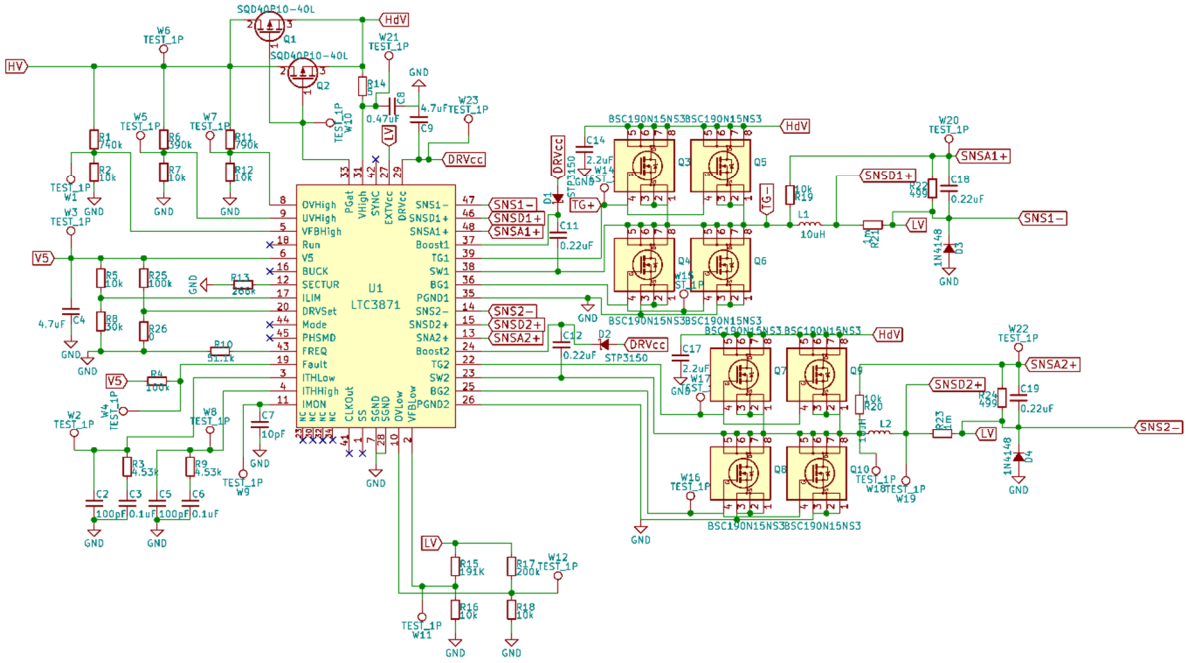

Figure A1. The schematic drawing of the DC-DC converter's printed circuit board. "HV" labels the high voltage input; "LV" labels the low voltage output.

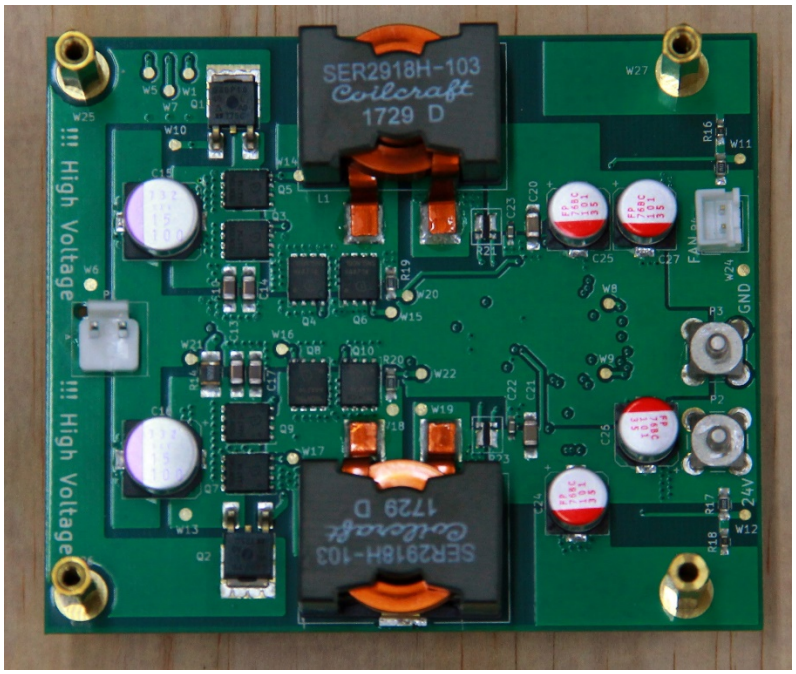

Figure A2. The photograph of the DC-DC converter's printed circuit board.

Before being utilized in the air, the DC-DC convertor was tested in the lab. The input voltage was 90 V and the output voltage was set to 24 V. The loading current was tuned from 8 A to 30 A. No component failure nor protection reaction was observed during the test. The efficiency is charted in Figure A3 with the efficiency value over 93% through the entire test.

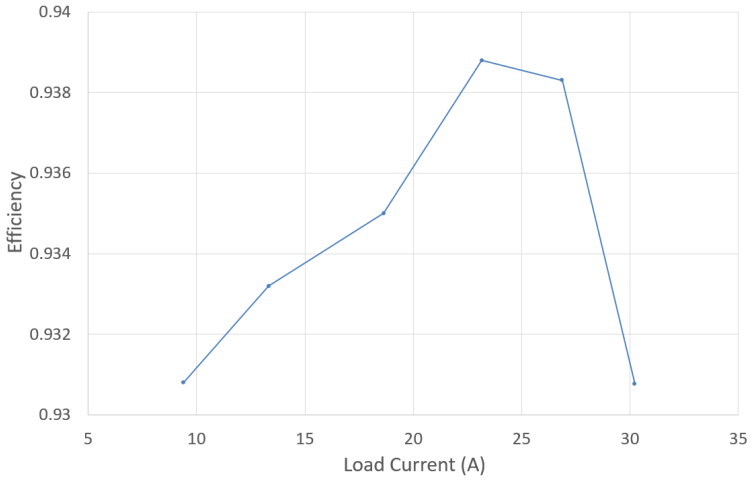

Figure A3. The efficiency of the DC-DC convertor under different load current.

References

1. Beekman, D.W.; Islam, M.S.; Dutta, A.K. Micro air vehicle endurance versus battery size. In Proceedings of the Micro- and Nanotechnology Sensors, Systems, and Applications II, Orlando, FL, USA, 5–9 April 2010.
2. Neitzke, K.-P. Rotary Wing Micro Air Vehicle Endurance. In Proceedings of the International Micro Air Vehicle Conference and Flight Competition IMAV, Toulouse, France, 17–20 September 2013; pp. 16–25.
3. Abdilla, A.; Richards, A.; Burrow, S. Power and endurance modelling of battery-powered rotorcraft. In Proceedings of the 2015 IEEE/RSJ International Conference on Intelligent Robots and Systems (IROS), Hamburg, Germany, 28 September–3 October 2015; pp. 675–680.
4. Gatti, M.; Giulietti, F.; Turci, M. Maximum endurance for battery-powered rotary-wing aircraft. *Aerosp. Sci. Technol.* **2015**, *45*, 174–179. [CrossRef]
5. Avanzini, G.; de Angelis, E.L.; Giulietti, F. Optimal performance and sizing of a battery-powered aircraft. *Aerosp. Sci. Technol.* **2016**, *59*, 132–144. [CrossRef]
6. Abdilla, A.; Richards, A.; Burrow, S. Endurance Optimisation of Battery-Powered Rotorcraft. In *Towards Autonomous Robotic Systems*; Lecture Notes in Computer Science; Springer: Cham, Switzerland, 2015; pp. 1–12. ISBN 978-3-319-22416-9.
7. Chang, T.; Yu, H. Improving Electric Powered UAVs' Endurance by Incorporating Battery Dumping Concept. *Procedia Eng.* **2015**, *99*, 168–179. [CrossRef]
8. Roberts, J.F.; Zufferey, J.C.; Floreano, D. Energy management for indoor hovering robots. In Proceedings of the 2008 IEEE/RSJ International Conference on Intelligent Robots and Systems, Nice, France, 22–26 September 2008; pp. 1242–1247.
9. Verbeke, J.; Hulens, D.; Ramon, H.; Goedeme, T.; De Schutter, J. The design and construction of a high endurance hexacopter suited for narrow corridors. In Proceedings of the 2014 International Conference on Unmanned Aircraft Systems (ICUAS), Orlando, FL, USA, 27–30 May 2014; pp. 543–551.
10. Vu, N.A.; Dang, D.K.; Le Dinh, T. Electric propulsion system sizing methodology for an agriculture multicopter. *Aerosp. Sci. Technol.* **2019**, *90*, 314–326. [CrossRef]
11. Winslow, J.; Benedict, M.; Hrishikeshavan, V.; Chopra, I. Design, development, and flight testing of a high endurance micro quadrotor helicopter. *Int. J. Micro Air Veh.* **2016**, *8*, 155–169. [CrossRef]
12. Jung, S. Development of Path Planning Tool for Unmanned System Considering Energy Consumption. *Appl. Sci.* **2019**, *9*, 3341. [CrossRef]
13. Kim, S.-B.; Lee, S.-H. Battery Balancing Algorithm for an Agricultural Drone Using a State-of-Charge-Based Fuzzy Controller. *Appl. Sci.* **2020**, *10*, 5277. [CrossRef]
14. Lin, C.E.; Supsukbaworn, T. Development of Dual Power Multirotor System. *Int. J. Aerosp. Eng.* **2017**, *2017*, 1–19. [CrossRef]
15. Mukhopadhyay, S.; Fernandes, S.; Shihab, M.; Waleed, D. Using Small Capacity Fuel Cells Onboard Drones for Battery Cooling: An Experimental Study. *Appl. Sci.* **2018**, *8*, 942. [CrossRef]
16. Kiribayashi, S.; Ashizawa, J.; Nagatani, K. Modeling and design of tether powered multicopter. In Proceedings of the 2015 IEEE International Symposium on Safety, Security, and Rescue Robotics (SSRR), West Lafayette, IN, USA, 18–20 October 2015; pp. 1–7.
17. Samarathunga, W.; Wang, G.; Wang, S. Heavy Payload Tethered Hexaroters for Agricultural Applications: Power Supply Design. *International Research Journal of Engineering and Technology.* **2015**, *2*, 641–645.
18. Wang, K.-Y.; Lee, P.-H.; Hung, S.-K. Optimum electric cable selection for kite-like unmanned aerial vehicle. In Proceedings of the 2015 IEEE International Conference on Advanced Intelligent Mechatronics (AIM), Busan, Korea, 7–11 July 2015; pp. 1537–1540.

19. Zikou, L.; Papachristos, C.; Tzes, A. The Power-over-Tether system for powering small UAVs: Tethering-line tension control synthesis. In Proceedings of the 2015 23rd Mediterranean Conference on Control and Automation (MED), Torremolinos, Spain, 16–19 June 2015; pp. 681–687.
20. Samarathunga, W.; Wang, G.; Wang, S. Vehicle Design of Tethered Hexaroters for Heavy Payload Applications. In Proceedings of the 2015 IEEE International Conference on Computational Intelligence & Communication Technology, Ghaziabad, India, 13–14 February 2015; pp. 554–556.
21. Vishnevsky, V.; Meshcheryakov, R. Experience of Developing a Multifunctional Tethered High-Altitude Unmanned Platform of Long-Term Operation. In *Interactive Collaborative Robotics*; Lecture Notes in Computer Science; Springer: Cham, Switzerland, 2019; pp. 236–244. ISBN 978-3-030-26118-4.
22. Samarathunga, W.; Wang, G.; Wang, S. Auxiliary Power Unit Evaluation for Tethered UAV. *Int. J. New Technol. Res. IJNTR* **2016**, *2*, 72–75.
23. Wang, G.; Samarathunga, W.; Wang, S. Uninterruptible Power Supply Design for Heavy Payload Tethered Hexaroters. *Int. J. Emerg. Eng. Res. Technol.* **2016**, *4*, 16–21.
24. Vishnevsky, V.; Tereschenko, B.; Tumchenok, D.; Shirvanyan, A. Optimal Method for Uplink Transfer of Power and the Design of High-Voltage Cable for Tethered High-Altitude Unmanned Telecommunication Platforms. In *Distributed Computer and Communication Networks*; Communications in Computer and Information Science; Springer: Cham, Switzerland, 2017; pp. 240–247. ISBN 978-3-319-66836-9.
25. Leishman, J.G. *Principles of Helicopter Aerodynamics*; Cambridge University Press: Cambridge, UK, 2003; ISBN 0521523966.
26. [PMEL] Design and Implement of a Tether-Powered Hexacopter for Long Endurance Missions. Available online: https://youtu.be/WHNUWNx-FfY (accessed on 7 December 2021).
27. CWB Observation Data Inquire System. Available online: https://e-service.cwb.gov.tw/HistoryDataQuery (accessed on 7 December 2021).